Comparison of Surface Wind Stress Anomalies over the Tropical Pacific Simulated by an AGCM and by a Simple Atmospheric Model

Ni Yunqi (倪允琪)
Department of Atmospheric Sciences, Nanjing University, Nanjing 210093
S. E. Zebiak and *M. A. Cane*
Lamont–Doherty Earth Observatory of Columbia
University, Palisades, N. Y. 10964, U.S.A.
D. M. Straus
Center for Ocean–Land–Atmosphere Studies,
Calverton, MD 20705–2425, U.S.A.
Received May 15, 1995; revised July 16, 1995

ABSTRACT

In this paper, surface wind stress anomalies over the tropical Pacific simulated by an AGCM and by a simple atmospheric model are compared with observed. The AGCM is the higher resolution global spectral model–COLA R40 model and the simple atmospheric model is the atmospheric component of the Cane–Zebiak coupled ocean–atmosphere model.

The results show that the wind stress anomalies simulated by both the COLA R40 and the simple model have captured the main features of observation but the x component in the CZ model is closer to that in observation than that in the COLA model, and the correlation coefficients between simulated SSTA from the CZ model and observed for Nino indices are higher than those from the COLA model.

Key words: Wind stress anomaly, Simple model, Global spectral model, Simulation

I. INTRODUCTION

An increasing supportive evidence shows that ENSO is the result of strong coupling between the ocean and the atmosphere in the tropics. Furthermore, there are two kinds of dynamic models which are coupled GCMs and simple coupled models (it refers to as intermediate model in McCreary's paper (1991)) have been used to predict ENSO events (Cane, 1991; Cane and Zebiak, 1987; Cane et al., 1986; Graham et al., 1992; Latif et al., 1992). Especially, a simple coupled model developed by Cane and Zebiak (1987, hereafter refers to as the CZ coupled model), which is able to capture broad aspects of interaction between ocean and atmosphere (Cane and Zebiak, 1987, 1988), has operationally predicted ENSO events during recent years. However, many coupled GCMs have had difficulty in simulating realistic ENSO events (McCreary, 1991) although Lau et al. (1992) and Philander et al. (1992) have used the GFDL GCMs to simulate oscillations like ENSO.

Why have coupled GCMs had difficulty in producing ENSO–like oscillations while simple coupled models can do it? One of main reasons in coupled GCMs develops climate drift which results from errors in model physics while the simple coupled models (here, simple coupled models are defined as the model like the CZ coupled model) avoid this problem effectively by building a climatological state directly into the system (in common, they are anomaly models). This kind of simple coupled models are sophisticated enough to produce

realistic solutions which illustrate possible fundamental processes of air–sea interaction and they are also simple enough to be relatively easy to diagnose. However, they are limited and there are some shortcomings existing in this kind of simple models because of oversimplified physical and dynamical processes in these models (McCreary, 1991). Therefore, question is how to compare their simulation and prediction capability with the GCMs. Obviously, capability of atmospheric component is main aspect for determining simulation and prediction of coupled models. Goswami and Shukla (1991) have also revealed that errors in the CZ coupled model mainly come from atmospheric component. Therefore, comparison of wind stress anomalies over the tropical Pacific simulated by AGCM with those by a simple atmospheric model is first needed in order to further understand simulation and prediction capability and characteristics of these two different coupled models.

In this paper, the structure of the COLA–R40 model and the CZ model are described in Section 2. The comparison of wind stress anomaly simulated by the COLA–R40 model with that by the CZ model is displayed in Section 3. The low– frequency characteristics of simulated wind stress anomalies by these two models are discussed in Section 4. Comparison of SSTA simulated by the CZ ocean model driven by the wind stress anomalies from the COLA model and the CZ model and observed is presented in Section 5. The last section summarizes the results and discusses them.

II. THE STRUCTURE OF THE MODELS

1. *The Cane–Zebiak Simple Atmospheric Model*

The equations of the CZ model consist of the linear non–dimensional momentum equations written as follows:

$$\begin{aligned} \epsilon u - yv &= -p_x, \\ \epsilon v + yu &= -p_y, \\ \epsilon p + \nabla \cdot V &= Q, \end{aligned} \tag{1}$$

where p is the surface pressue, u and v respectively denote x and y component of surface wind anomaly.

Equation (1) is solved by using spectral decomposition in x, and finite differencing in y. It may be written as follows

$$V_{j-1} + \left(\frac{i\pi\Delta y^2 k}{2\epsilon} - 2 - \frac{\Delta y^2}{4} y_j^2 - \Delta y^2(\epsilon^2 + k^2)\right)V_j + V_{j+1} =$$
$$-\frac{\Delta y}{2}\tilde{Q}_{j-1} + \frac{i\pi\Delta y^2 k}{2\epsilon}{}_j\tilde{Q}_{j+1} + \frac{\Delta y}{2}\tilde{Q}_j \qquad j = 1,N \tag{2}$$

where Δy is the grid spacing and N is the total number of interior grid points in y. The lateral boundary condition in (2) is that $V = 0$ at the pole (i.e. $V_{j=1}$ and $V_{j=N} = 0$).

Once the spectral coefficients $\{V_j\}$ are found, the spectral coefficients $\{U_j\}$ are obtained using

$$(k^2 + \epsilon^2)U_j = \epsilon y_j V_j / 2 + \frac{ik}{2\triangle y}(V_{j+1} - V_{j-1}) + ik\tilde{Q}_j \qquad j = 1,N \tag{3}$$

In these calculation, the domain in y is from −7.9 (79°S) to +7.9 (79°N) and $y = 0.2$ (~ 200 km). The spectral decomposition is done using a 64–point FFT and the domain in x is the full 360 longitudes, give a spectral resolution (in x) of about 600 km. The diabatic heating

Q is calculated by a parameterization which is related to SSTA, convergence in the lower troposphere, and feedback to surface wind. These feedback processes between latent heat released in areas of organized convection and the wind field are available for the tropical region.

The above model is integrated from 1979 to 1983 with observed SSTA.

2. *The Higher Resolution Global Spectral Model–COLA R40 Model*

The AGCM being used in this study is a modified version of the National Meteorological Center (NMC) global spectral model. The detailed formulation and the initialization procedures and boundary conditions are described in Sela (1980) and Kinter et al. (1988).

Model prediction employs the primitive equations of motion and a prognostic equation for the mixing ratio of water vapor. The equation for the vertical component of velocity is replaced by a diagnostic relationship on the assumption that motions are in hydrostatic equilibrium.

This model has 18 layers in the vertical incorporated with a modified sigma vertical coordinate and horizontal resolution with rhomboidal truncation at wave number 40. The semi–implicit scheme is used for time integration.

The physical processes in this model include a parameterization for the absorption of solar radiation, a radiative transfer calculation for the long–wave components of terrestrial radiation, a boundary layer momentum and heat flux parameterization based on the mixing length theory of Monin and Obukhov and a parameterization for gravity wave drag, a three layer soil temperature formulation for the surface heat balance, a ground hydrology budget for soil moisture. An interactive cloud scheme and a simplified version of simple biosphere model are incorporated in the AGCM. Additionally, momentum, heat and moisture diffusion (horizontal and vertical) are considered.

The model is initialized using a two–iteration, non–linear normal mode scheme. The boundary conditions used are climatological, seasonally varying surface conditions derived from recently available sources and ozone mixing ratio derived from observed seasonal mean values.

The simulation is made using the above AGCM with realistic sea surface temperature from 1979 to 1983.

III. WIND STRESS ANOMALIES OVER THE TROPICAL PACIFIC SIMULATED BY THE COLA R40 MODEL AND BY THE CANE–ZEBIAK ATMOSPHERIC MODEL

In this study, avoiding the spurious topographic effect on surface wind stress in the spectral model, the wind stress at 1000 hPa is recalculated by using the wind at 1000 hPa in COLA R40 model and drag coefficient is 0.0329. Then, surface wind stress anomalies over the tropical Pacific from the mean of the five year integration (1979–1983) for the COLA R40 model are obtained. However, the same wind stress from the CZ model is calculated by using the same formula as that in the COLA model.

The four–pole low pass filter (Kaylor, 1977) is used to filter the observed and simulated wind stress anomalies with cutting the signals with the frequency higher than that 1 / 5 months (half power). This means the signals with the frequency lower than frequency of seasonal variability (i.e. semi–annual, annual and biennial oscillation signals and so on are kept).

The longitude–time cross sections of the x component of wind stress anomalies along the equator simulated by the COLA AGCM and the CZ model and observation are respectively shown in Fig.1.

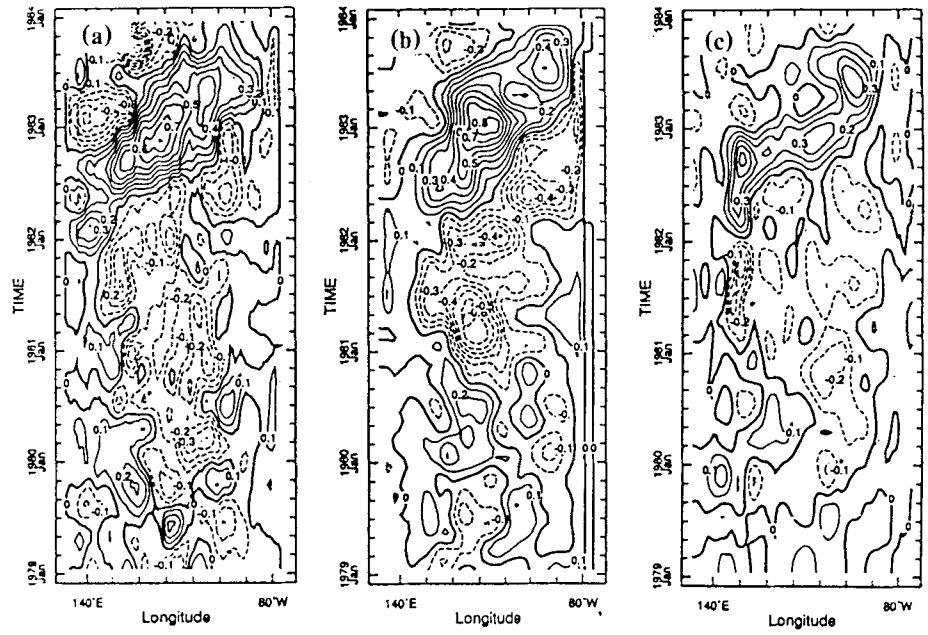

Fig. 1. The longitude–time cross-section of the x component of wind stress anomalies along the equator.

Comparing Fig. 1(a) with Fig. 1(b), we can find that in simulation from the CZ model, positive anomalies dominate over west of dateline and the area from 110°W to 160°W from Jan. 1979 to Dec.1979 and over the central Pacific from Dec. 1979 to Oct.1981. Although the simulation over the above areas is not consistent with observation well, you can find correspondence between simulation and observation in other areas. Especially, the negative anomaly area since Oct. 1980 and the positive anomaly area since Feb. 1982 capture the main features appearing in observation very well, which the positive anomaly propagates eastward from the western–central Pacific in Feb. 1982 to eastern Pacific in Dec. 1983, although their starting time is little earlier than observation.

Comparing Fig. 1(a) with Fig. 1(c), it is clear that simulated zonal flow along the equator in the COLA model, in general, is weaker than observation which is common discrepancy in all the AGCM (McCreary et al., 1991) but anomaly patterns and position of the centers in simulation are basically similar to those in observation. From Jan. 1979 to March 1982, negative anomalies dominate over the central–eastern tropical Pacific and positive anomalies are located in the western Pacific from Jan. 1979 to March 1982 in observation. All these characteristics of zonal flow are basically reproduced by the COLA R40 model except for a few anomaly center locations. From Jan. 1980 to Oct. 1980, positive anomalies dominate in west of 160°W, which is extended slightly to the east of its position in the observation. Since Aug. 1980 until March 1982, all the tropical Pacific is occupied by negative wind stress anomalies in both simulation and observation. In Jan. 1982, the positive anomalies start to appear over the western Pacific in both simulation and observation. In simulation, then, the positive anomalies gradually propagate eastward and the positive anomalies are appearing over all the tropical Pacific in June 1982 while in observation, the positive anomalies appear over all the tropical Pacific in March 1982 when is earlier than simulation. Note that in simulation, a negative anomaly area is faster propagated eastward from the western equatorial Pacific to cen-

tral–eastern equatorial Pacific since Jan. 1983 until March 1983, which this phenomenon is not appearing in observation.

It is noteworthy that the y component of simulated wind stress anomalies along the equator by the COLA R40 model strongly bears resemblance to that in observation (not shown) except for some higher frequency signals existing in observation. Especially, negative anomalies since Nov. 1981 until Aug. 1982 and positive anomalies since timated 1982 until the end of 1983 dominated along the equator in simulation, which are consistent with observation very well. In the CZ model, however, the y component of wind stress anomalies along the equator (not shown) is much weaker than that in observation but it still captures the main features in observation.

Fig.2 represents correlation coefficients between the x component of wind stress anomalies from the COLA model and observation. Fig. 2 shows that the area where correlation coefficients are greater than 0.3 (it is statistically significant at 0.05 level) is located in the zone along the equator from 160°E to 100°W and then extended northwestward to Asian monsoon area and eastward to the coast of Latin America from the north of the equator but the correlation coefficients are negative off the coast of South America. The maximum coefficient reaches over 0.8 located over near the dateline and off the coast of Latin America. The correlation map of the y component (not shown) shows that the area where coefficients are greater than 0.3 almost occupied the zone to north of the equator from the dateline to the coast of South America, Asian monsoon area and some areas located in subtropics of the Southern Hemisphere. However, the coefficients in south of the equator are lower even negative which reflects the ITCZ in simulation south too far away from position in observation and large error existing in simulation off the coast of South America where is affected by the spurious topography of Andes mountain in the spectral model. However, why the negative coefficients appear in the central Pacific to the north of the equator is not clear yet.

Fig.3 gives correlation coefficients between the x component of simulated wind stress anomalies from the CZ model and observation. Fig.3 shows that the zone where correlation coefficients for the x component are greater than 0.3 is along the equator from the western Pacific to the eastern Pacific and negative coefficients are occupied in all the area to north of 10°N and to south of 10°S. The area where the correlation coefficients for the y component(not shown) are greater than 0.3 is also along the equator, the central Pacific

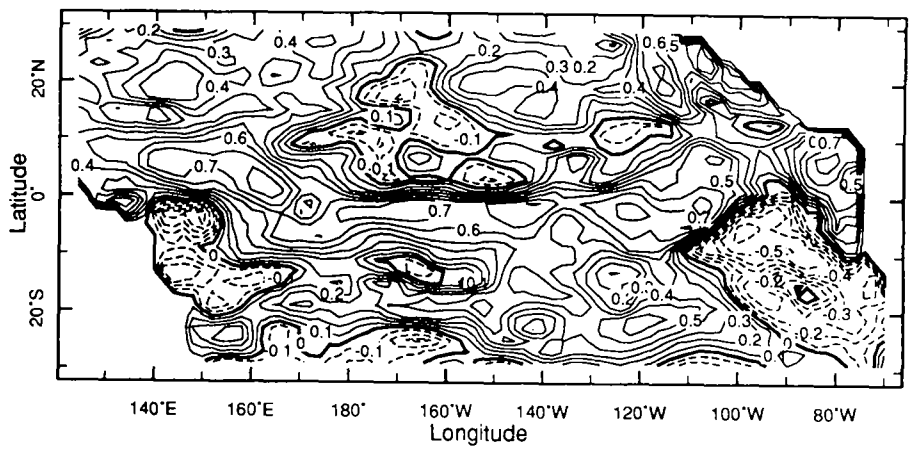

Fig.2. Correlation coefficients between the x component of wind stress anomalies from the COLA model and from observation.

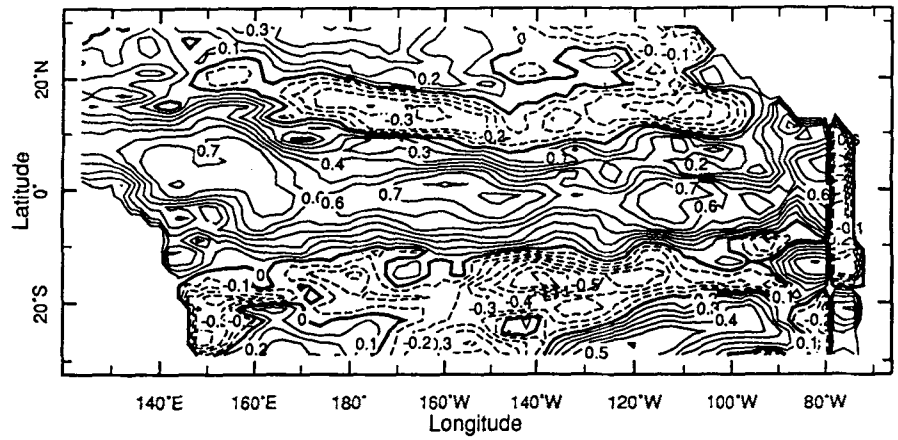

Fig. 3. As in Fig. 2 except for the CZ model.

to the south of the equator and part of Asian monsoon area. However, the maximum coefficients for the x component reaches over 0.8 and for the y component(not shown) reaches over 0.9. These facts indicate that simulation capability of the CZ model to wind stress anomalies concentrates on the area near the equator, especially the central equatorial Pacific.

Comparing Fig.2 with Fig.3, we can find that in the CZ model, the statistically significant area (correlation coefficients are greater than 0.3 at significant level 0.05) for the x component of wind stress anomalies along the equator is larger than that in the COLA model, however, the significant area not only situates along the equator but also extends northwestward to Asian monsoon area and other regions in the COLA model. The higher coefficient area for the y component (not shown) is mainly located in the central tropical Pacific in the CZ model while in the COLA model, the higher coefficient area not only covers the central tropical Pacific but also in all the Asian monsoon region.

Fig.5 gives correlation coefficients between the x component of simulated wind stress anomalies by the CZ model and Nino3 indices. We can find that the characters in Fig.5 are very similar to those in Fig.4, that is, the positive and negative areas along the equator in Fig.5 are consistent with those in Fig.4 except for southeast of the tropical Pacific and near the dateline. Note that the maximum correlation coefficient in Fig.5 is larger than that in Fig.4 and Fig.6, which reaches over 0.9 because all the signals in the CZ model are low-frequency while both observation and simulation in the COLA model involve higher and lower frequency signals.

Fig.6 shows correlation coefficients between the x component of simulated wind stress anomalies by the COLA model and observed Nino3 indices. It is interesting that the x component of wind stress anomalies along the equator or near the equator and east of 130°W in the COLA R40 model has positive relationship with Nino3 indices, which indicates that westerly anomalies increase Nino3 indices and easterly anomalies decrease Nino3 indices but centers of positive relation are located to the south of equator; however, the correlation coefficients are reverse in north and south of this positive area, which reflects that westerly anomalies decrease the Nino3 indices and easterly anomalies increase Nino3 indices. It is noteworthy that the relation patterns in Fig.6 are basically similar to the patterns in Fig.4 except for the area located in southeast of the tropical Pacific (see Fig.4).

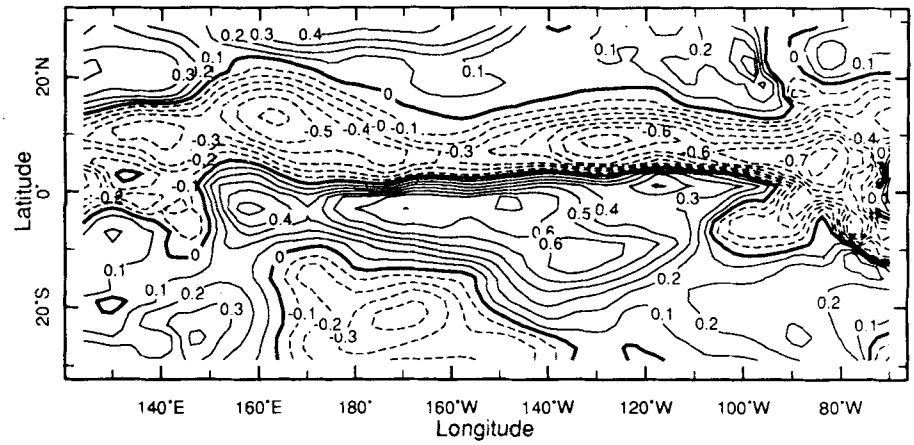

Fig. 4. Correlation coefficients between the x component of observed wind stress anomalies and observed Nino index.

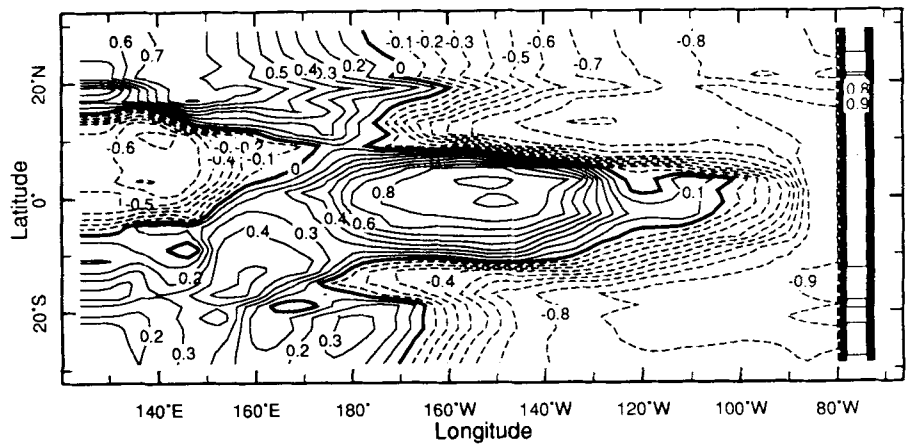

Fig. 5. As in Fig. 4 except for the CZ model.

Standard deviations of the x component wind stress anomalies observed and simulated by the CZ model and the COLA model are respectively represented in Figs. 7, 8 and 9.

Comparing Fig.7 with Fig.9, we can find that basic characteristics of wind stress anomalies over subtropics in observation are reproduced by the COLA model but they are overestimated in the subtropics and underestimated in the tropics. The correspondence between simulation and observation over the subtropics is clear evidence of basic success of simulated wind stress anomalies over the subtropics by the COLA model. However, deficiencies which seem to exist in the representation of the x component of simulated wind stress anomalies in the COLA model especially over the equator or near the equator may be noted, which the standard deviation for the x component along the equator is much smaller than that in observation.

In Fig.8, we still can find correspondence between Fig.8 and Fig.7 over the subtropics although their difference is apparant especially the amplitudes are underestimated in Fig.8. It is noteworthy that standard deviation for the x component along the equator or near the

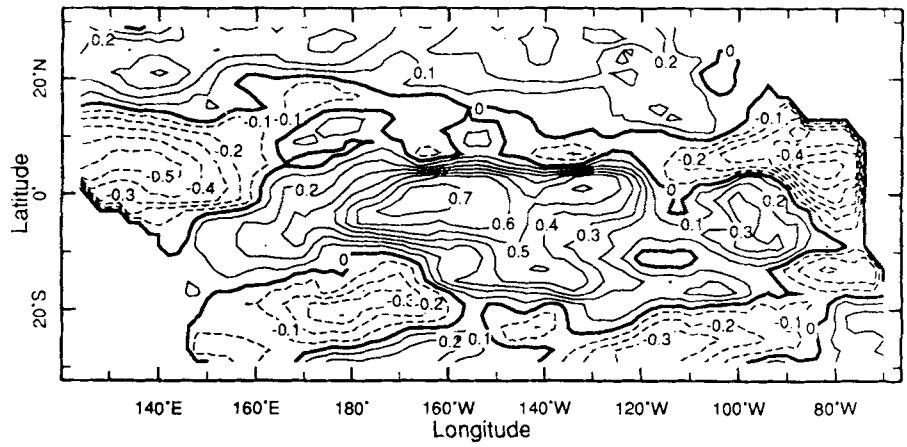

Fig. 6. As in Fig. 5 except for the COLA model.

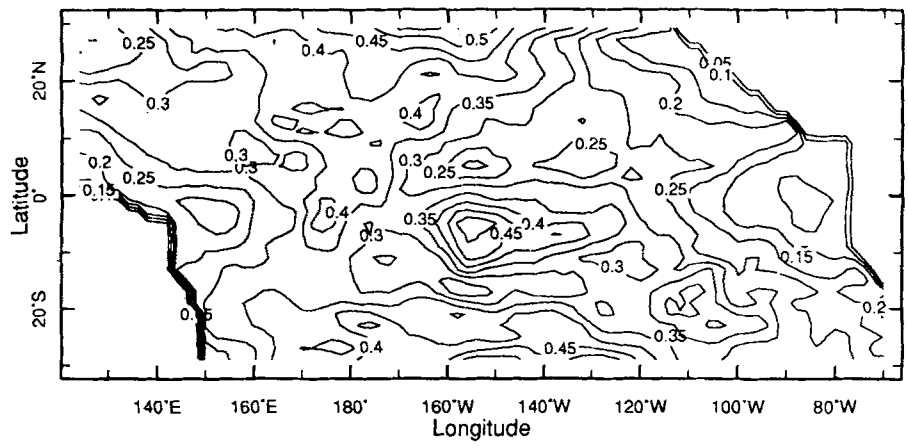

Fig. 7. Standard deviation of the x component of observed wind stress anomalies from FSU.

equator in simulation basically captures the characters of observation including the amplitude of the standard deviation although their amplitudes are smaller than observation.

IV. ANALYSIS AND COMPARISON OF THE SIMULATED SSTA IN THE TROPICAL PACIFIC BY THE CANE–ZEBIAK OCEAN MODEL DRIVEN BY SIMULATED AND OBSERVED WIND STRESS ANOMALIES

1. *Brief Description of the Ocean Model*

The ocean model has been presented in detail by Zebiak (1984) and will be briefly described here.

The dynamics of the model begins with the linear reduced–gravity model. Such model produces only depth–averaged baroclinic currents, but the surface current is usually dominated by the frictional (Ekman) component. Therefore, a shallow frictional layer of constant depth (50 m) is added to the simulated surface intensification of wind–driven currents in the real ocean. The dynamics of this layer is also kept linear, but only by using Rayleigh friction

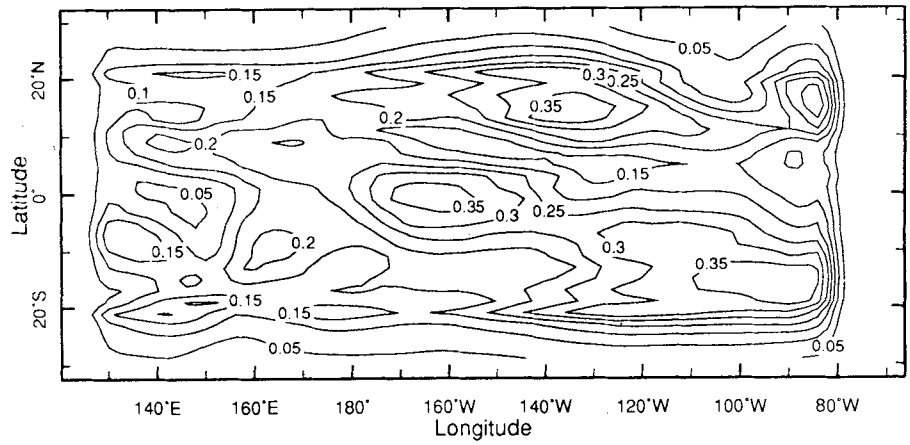

Fig.8. As in Fig. 7 except for the CZ model.

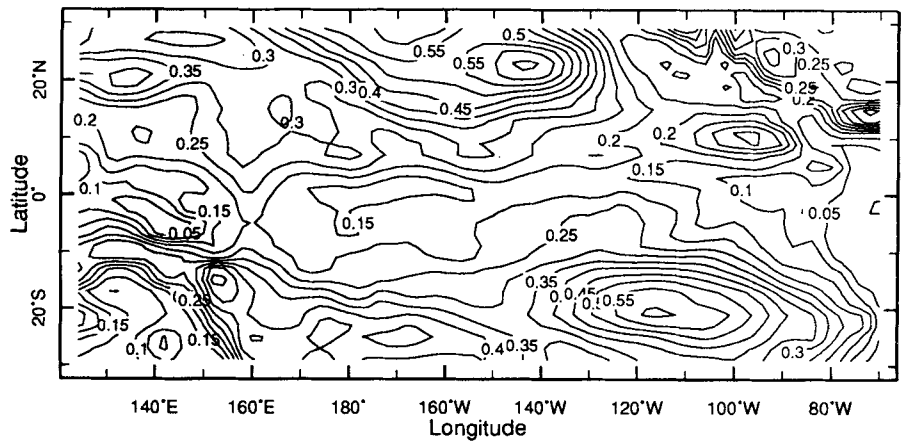

Fig.9. As in Fig. 7 except for the COLA model.

to stand for nonlinear influence at the equator. The surface layer pressure gradient varies only with the thermocline depth in this model, which neglects the influence of any temperature changes occurring in the surface layer alone.

The governing equation describing the evolution of temperature anomalies in the model surface layer includes three–dimensional temperature advection by both the specified mean currents and the calculated anomalous currents. The assumed surface heat flux anomaly is proportional to the local SST anomaly, acting always to adjust the temperature field toward its climatological mean state, which is specified from observation.

The above ocean model is integrated from 124°E to 80°W and from 29°N to 29°S driven by the simulated wind stress anomalies by the COLA R40 model and the CZ model and observed wind stress anomalies for 5 years since Jan. 1979 until Dec. 1983.

2. *Analysis and Comparison of the Simulated SSTA in the Tropical Pacific*

At first, the simulation capability of the Cane–Zebiak ocean model is tested by using ob-

served wind stress anomalies from FSU.

The dot lines shown in Fig. 10 present simulated Nino3 indices by observed wind stress anomalies from FSU.

The Nino3 index is defined as averaged SSTA in the areas from 5°N to 5°S and from 150°W to 90°W.

Fig.10 (a) shows that the main tendency of the Nino3 index variation from Jan. 1979 to Dec. 1983 is reproduced well by the observed wind stress anomalies. The correlation coefficients between the simulated Nino3 index and observed are 0.82.

Fig. 11 gives the simulated and observed SSTA along the equator from Jan. 1979 to Dec. 1983. Comparing Fig.11 (a) with Fig.11 (b), it is clear that the ocean model captures the main

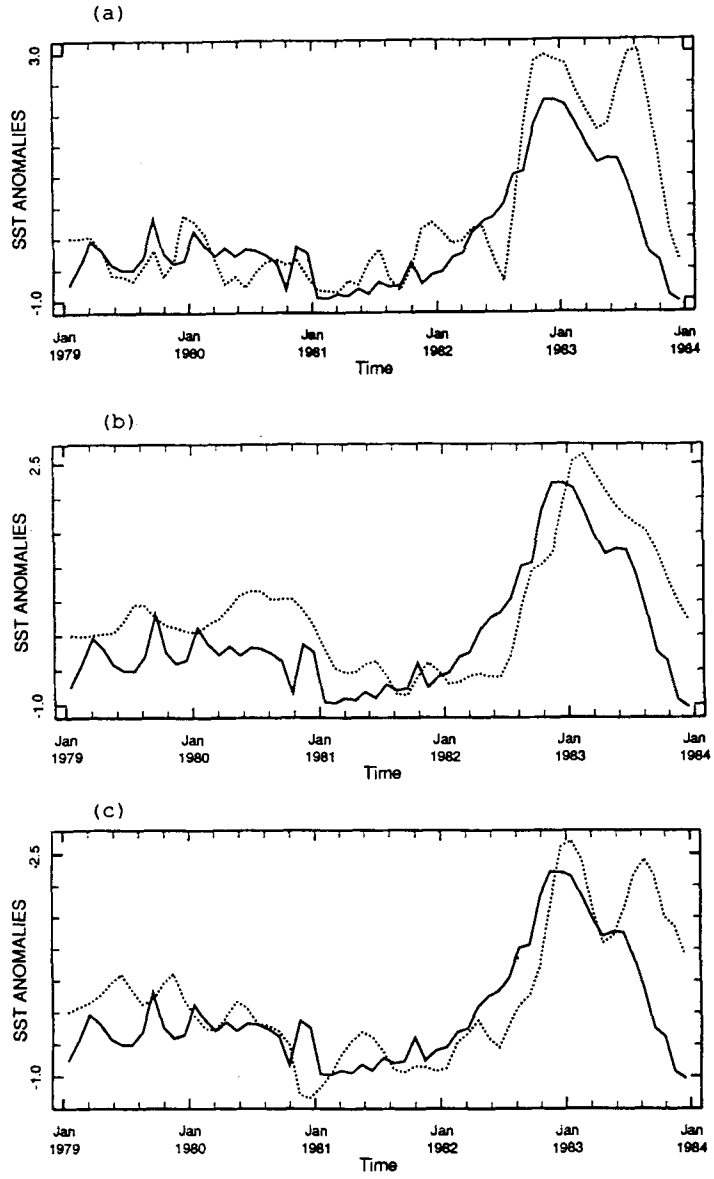

Fig.10. Variation of Nino3 index in the ocean model driven by observed and simulated wind stress anomalies: (a) observation; (b) the CZ model; (c) the COLA model.

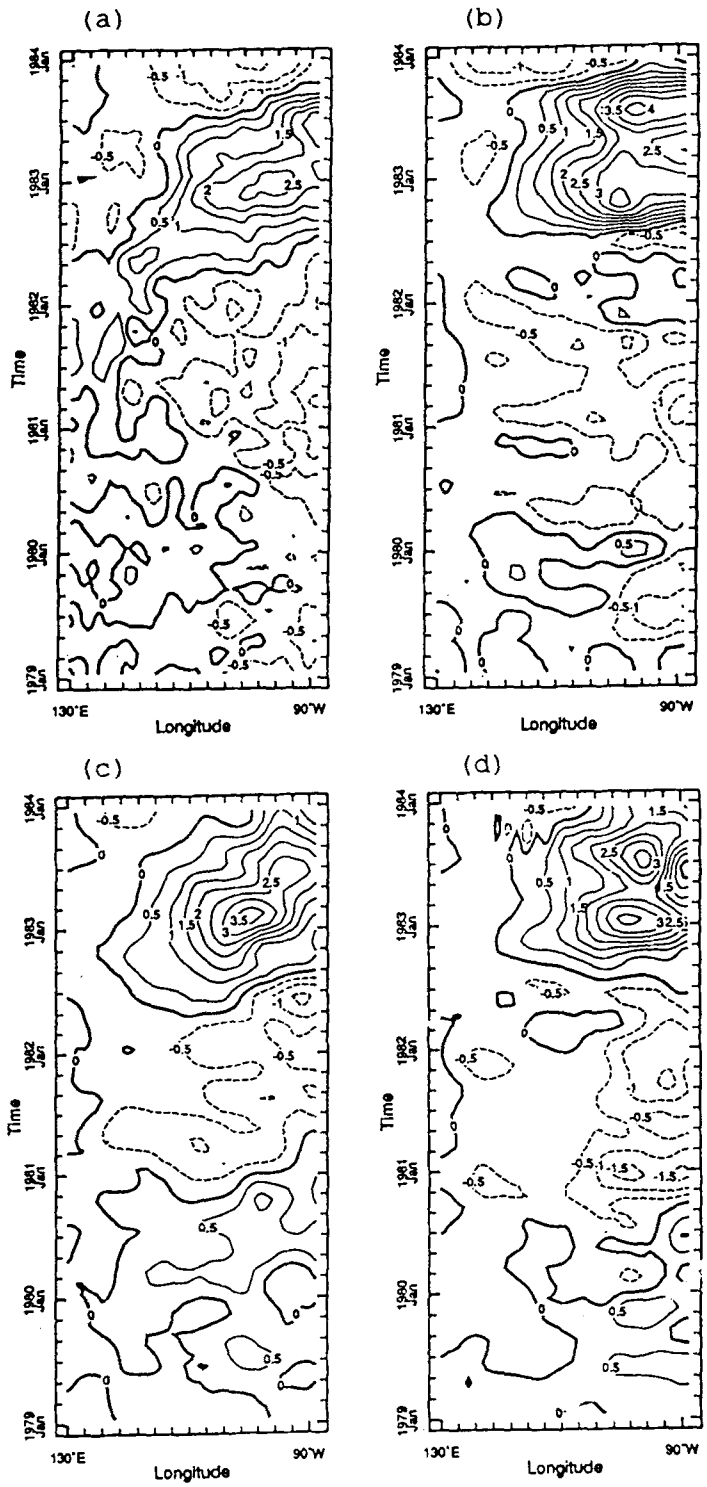

Fig.11. The longitude–time cross–section of SSTA along the equator: (a) observation; (b) simulated by observed wind stress anomalies; (c) simulated by the wind stress anomalies from the CZ model; (d) as in (c) except for the COLA model.

characteristics of observed SSTA in the central–eastern Pacific along the equator but in the central–western Pacific SSTA along the equator is not simulated well, which are consistent with results shown in Fig.10.

The correlation coefficients between SSTA simulated by observed wind stress anomalies and observed SSTA are shown in Fig.12(a). Fig.12(a) clearly shows that the area where correlation coefficients are greater than 0.5 is located in the central–eastern Pacific and the north and south of the equator in the western Pacific. This result indicated that the capability of simulated SSTA of this ocean model is strong in the central–eastern Pacific. This conclusion shows that it is reasonable of using the Cane–Zebiak ocean model to analyze and compare the simulated wind stress anomalies by the COLA and the CZ models.

Figs.10 (b) and (c) show that main variation characters of the Nino3 index are reproduced by both models. The correlation coefficients between simulated by the CZ and the COLA models and observed Nino3 index respectively reach 0.76 and 0.67.

It is noteworthy that comparing simulated SSTA along the equator from the ocean model driven by observed wind stress, simulated wind stress anomalies from the CZ and the COLA model (see Fig.11), we can find that all the simulated SSTAs along the equator are consistent with observed SSTA except for intensity during the 82–83 El Nino period but there is a positive anomaly area in the central–eastern Pacific since Feb. 1980 until Dec. 1980 in the simulation from the CZ model, which is not consistent with observed and other results. Furthermore, comparing Fig.11 (b) with Fig.11 (d), the patterns and intensity from the COLA model are in agreement well with those from observed wind stress anomalies. These facts indicate that the simulated SSTA from the COLA model is comparable of those from observed and the CZ model although the correlation coefficients between simulated from the COLA model and observed for Nino indices are lower than those from the CZ model.

Fig.12 (b) and (c) respectively give correlation coefficients between SSTA simulated by the COLA and the CZ models and observed SSTA. Fig.12 (c) clearly shows that higher correlation coefficients are appearing in the eastern tropical Pacific in the COLA model and the pattern in the COLA model is very similar to that in the observation (see Fig.12 (a)). However, the higher coefficients are appearing in the central tropical Pacific and off the coast of South America and the highest coefficient in the CZ model is higher than that in the COLA model. These results suggest that the COLA model has strong simulation capability in the eastern Pacific region and the CZ model in the central Pacific. Obviously, SSTA in the western Pacific isn't produced well, which reflects that simulation capability of the ocean model is weak in the western Pacific.

V. DISCUSSION AND CONCLUSIONS

The simulated wind stress anomalies by an AGCM–COLA R40 model and by a simple atmospheric model–the Cane–Zebiak model have been analyzed and compared. The conclusions are the following:

1) patterns of the wind stress anomalies simulated by the COLA R40 model are closer to those in observation especially the y component in the COLA model is consistent with observation well but the x component is weak compared with observation; the wind stress anomalies simulated by the CZ model capture the main features in observation especially the x component but y component in the CZ model is weak compared with the observation. These results summarized in Table 2.

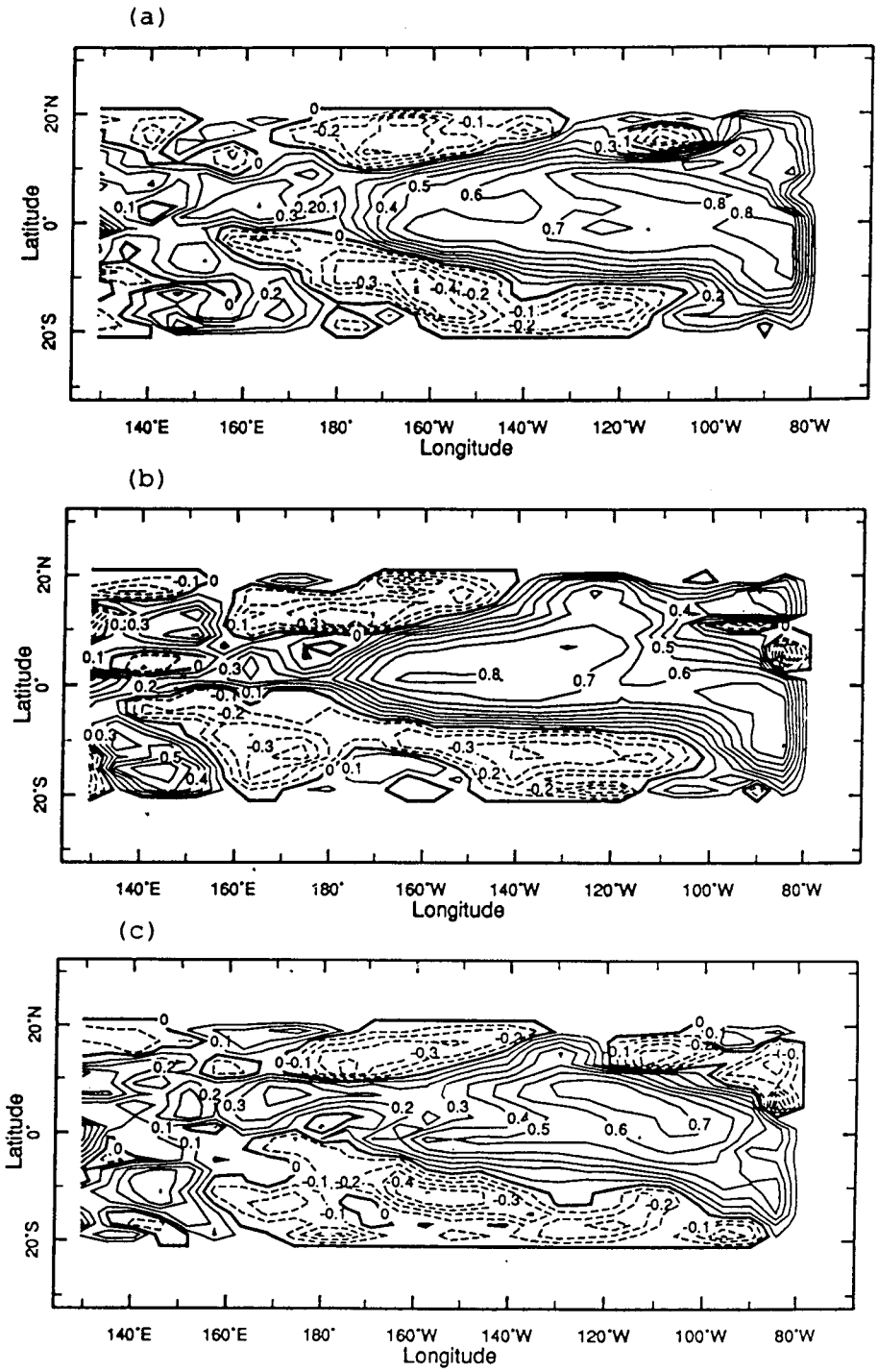

Fig. 12. Correlation coefficients between observed SSTA and simulated SSTA: (a) by observed wind stress anomalies; (b) by wind stress anomalies from the CZ model; (c) by wind stress anomalies from the COLA model.

2) in the COLA model, standard deviation of the x component of wind stress anomaly is overestimated in the subtropics and weak in the tropics compared with observation while the

y component is consistent with observation. However, standard deviation of the x component in the CZ model captures the main characters in observation especially along the equator but the y component is weak.

3) all the simulated SSTAs along the equator are consistent with observed SSTA except intensity during the 82–83 El Nino event. The simulated SSTA from the COLA model is comparable of those from observed and the CZ model although the correlation coefficients between simulated from the CZ model and observed for Nino indices are higher than those from the COLA model. These results are summarized in Table 1.

Table 1. Correlation Coefficients and RMSE between Nino Index by Simulated and by Observed (1979–1983)

Ocean Model driven by	COLA R40 Wind Stress		ZCAM Wind Stress		Observed Wind Stress	
	R	RMSE	R	RMSE	R	RMSE
Nino3 (120°W, Eq.)	0.72	0.753	0.76	0.701	0.82	0.805
Nino1 (87°W, 7°S)	0.38	1.255	0.87	0.765	0.86	0.698
Nino4 (175°W, Eq.)	0.02	0.451	0.49	0.397	0.48	0.351

Table 2. Correlation Coefficients and RMSE between TW1, TW2 by Simulated and by Observed (1979–1983)

Correlation Coefficient				RMSE			
TW1		TW2		TW1		TW2	
COLA	ZCAM	COLA	ZCAM	COLA	ZCAM	COLA	ZCAM
0.84	0.77	0.57	0.80	0.084	0.089	0.192	0.177

* TW1 defined as averaged x component of wind stress in the area from 5°N to 5°S and from 135°E to 180;

* TW2 defined as averaged x component of wind stress in the area from 5°N to 5°S and from 175°W to 140°W;

4) Some common and poor features result from known deficiencies of the ocean model–in particular, its inability to capture subtropical SST variability, due to the simplified surface heat flux formulation.

We would like to thank for supports from director of COLA, Prof. J. Shukla, Mr. L. Marx, Mr. M. Fennessy and Mrs. M. A. Huntley in COLA, Maryland University and Dr. L. Rosen in LDGO, Columbia University.

REFERENCES

Cane, M. A., S. E. Zebiak and S. C. Dolan (1986), Experimental forecasts of El Nino, *Nature*, **321:** 827–832.

Cane, M. A. and S. E. Zebiak (1987), Prediction of El Nino event using a coupled models; Atmospheric and Oceanic Variability, H. Cattle, Ed., Royal Meteorological Society, 153–181.

Cane, M. A. and S. E. Zebiak (1988), Dynamic forecasts of the 1986–1987 ENSO with a coupled model, *Proc, of the 13th Annual Climate Diagnostic Workshop, NOAA*, 278–282.

Cane, M. A. (1991), Forecasting El Nino with a geophysical model, Teleconnections linking worldwide climate anomalies, M. Glantz, R. W. Katz, and N. Nicholls (Eds.), Cambridge University Press.

Goswami, B. N. and J. Shukla (1991), Predictability of a coupled ocean atmosphere model, *J. of Climate*, **4:** 3–22.

Graham, N. E., T. P. Barnett and M. Latif (1992), Considerations of the predictability of ENSO with a low–order coupled model, *TOGA notes*, **7:** April, 11–15.

Kaylor, R. E. (1977), Filtering and decimation of digital time series, Technical Note BN 850, Institute for Physical

Science and Technology, University of Maryland.

Kinter, J. L., III, J, Shukla, L. Marx and E. K. Schneider (1988), A simulation of the winter and summer circulation with the NMC global spectral model, *J. A. S.*, **45:** 2486–2522.

Latif, M., A. Sterl, E. Maier–Reimer, and M. M. Junge (1992), Structure and predictability of the El Nino / Southern Oscillation phenomenon, *J. Climate*, subm.

Lau, N.C., S.G.H. Philander, and M.J. Nath (1992), Simulation of El Nino / Southern Oscillation phenomena with a low–resolution coupled general circulation model of the global ocean and atmosphere, *J. Climate*, **5:** 284–307.

McCreary, Jr., J. P. and D. L. T. Anderson (1991), An overview of coupled ocean–atmosphere models of El Nino and the Southern Oscillation, *J. Geophys. Res.*, **96:** 3125–3150.

Philander, S.G.H., R.C. Pacanowski, N.C.Lau, and M.J. Nath (1992), Simulation of ENSO with a global atmospheric GCM coupled to a high–resolution, tropical Pacific ocean GCM, *J. Climate*, **5:** 308–329.

Sela, J. G. (1980), Spectral modeling at NMC, *Mon. Wea. Rev.*, **108:** 1279–1292.

Zebiak, S.E. (1984), Tropical atmosphere–ocean interaction and the El Nino / Southern Oscillation phenomena, Ph.D thesis, MIT, 261pp.